

## Surface texturing on SiC by multiphase jet machining with microdiamond abrasives

Liping Shi, Yu Fang, Qingwen Dai, Wei Huang & Xiaolei Wang

To cite this article: Liping Shi, Yu Fang, Qingwen Dai, Wei Huang & Xiaolei Wang (2018) Surface texturing on SiC by multiphase jet machining with microdiamond abrasives, Materials and Manufacturing Processes, 33:13, 1415-1421, DOI: [10.1080/10426914.2017.1401723](https://doi.org/10.1080/10426914.2017.1401723)

To link to this article: <https://doi.org/10.1080/10426914.2017.1401723>



Published online: 15 Nov 2017.



Submit your article to this journal [↗](#)



Article views: 21



View related articles [↗](#)



View Crossmark data [↗](#)



Citing articles: 1 View citing articles [↗](#)



# Surface texturing on SiC by multiphase jet machining with microdiamond abrasives

Liping Shi<sup>a,b</sup>, Yu Fang<sup>a</sup>, Qingwen Dai<sup>a</sup>, Wei Huang<sup>a</sup>, and Xiaolei Wang<sup>a,c</sup>

<sup>a</sup>College of Mechanical and Electrical Engineering, Nanjing University of Aeronautics and Astronautics, Nanjing, China; <sup>b</sup>College of Mechanical Engineering, Anhui University of Technology, Ma'anshan, China; <sup>c</sup>Jiangsu Key Laboratory of Precision and Micro-Manufacturing Technology, Nanjing, China

## ABSTRACT

The multiphase microabrasive jet machining is a new type of surface texturing technique using compressed air to accelerate the mixtures of abrasive and water to remove material. It is effective for surface texturing on different materials, and can also reduce the pollution and cost by recycling the microabrasive particles easily. Basing on this technique and using the micro synthetic diamond as the abrasive, a multiphase jet technique is developed for machining on silicon carbide (SiC) surfaces. The processing results are compared to other abrasives, and influences of the processing parameters such as jet distance, jet pressure, abrasive concentration, particle size, and jet angle are investigated experimentally. The improvement on machining quality and efficiency are confirmed.

## ARTICLE HISTORY

Received 16 August 2017  
Accepted 30 October 2017

## KEYWORDS

Abrasive; jet; micromachining; microstructure; multiphase; spiral-grooves; synthetic-diamond; texturing

## Introduction

Mechanical seals are essential shaft sealing components in rotary machineries. They are widely used in petrochemical industry, jet engines, aerospace and metallurgical industry to prevent the leakage of lubricants between dynamic and static rings.<sup>[1,2]</sup> The abrasion of rotating and stationary rings surfaces are critical which limits the reliability and durability of mechanical seals, particularly under the conditions of high speed and high contact pressure in modern industry. Over the past decades, surface texture has been proven to be an effective way to enhance the sealing performance and durability.<sup>[3–5]</sup>

Various materials including hard materials such as cemented carbide and silicon carbide, and soft materials such as carbon graphite and Polytetrafluoroethylene (PTFE), are often used for the rotating and stationary rings of mechanical seals to achieve a good mating performance.

To fabricate the surface textures with proper shape and dimensions, many machining techniques such as LIGA lithography, laser, electrochemical etching, and micromilling have been developed.<sup>[6–8]</sup> However, based on the mechanism of machining, every technique has its limitation as well as advantages. For example, the laser may result in heat affected zone on the surface, the electrical discharge machining and the electrochemical etching can do nothing with nonconductive materials such as silicon carbide, the microultrasonic machining is always associated with the reduction of machining precision caused by tool wear.

Microabrasive jet machining (MAJM), including microabrasive water jet machining and microabrasive gas jet machining, is also an effective method of material removal.<sup>[9–12]</sup> Compared with the other processing methods, the MAJM can be used to process a variety of materials, it

doesn't change the chemical and physical properties of the material and has no heat affected zone or residual stress on the processed surface.<sup>[13,14]</sup> Additionally, the gas jet machining can operate under the pressure below 1 MPa, much lower than that for water jet machining.<sup>[15,16]</sup> For the fabrication of micro structures, the abrasive particles of small size are necessary. However, it is easy to be released to the environment causing potential pollution problem, and is difficult to be recycled, which is costly to use the precious abrasives.<sup>[17]</sup>

Previously, Tsai et al.<sup>[18]</sup> used compressed air to accelerate the mixtures of abrasives, water and machining oil for surface polishing. Inspired by that, Su et al.<sup>[19]</sup> used green silicon carbide (GSC) as the abrasives, developed a multiphase microabrasive jet machining (M-MAJM) for surface machining. In M-MAJM process, the abrasives particles are mixed with a specific quantity of water, and then accelerated by compressed air to remove materials at specific areas, so that the particles can be reused by separating from water, and the jet flow could get relative high speed with regular compressed air. The M-MAJM performs well in processing of carbon graphite and stainless steel when using silicon carbide as abrasives. However, for fabricating microgrooves on silicon carbide (SiC), the processing efficiency is low, and the surface roughness on the bottom of microstructure is relative high because of the existence of unmachined "isolated islands." It is of great value in the engineering application to make further research to improve the machining efficiency and quality of M-MAJM on hard materials.

Therefore, in this paper, synthetic diamond (SD) is used as microabrasive, and the multiphase microdiamond jet machining (M-MDJM) is proposed for micromachining on SiC surface. The influences of jet distance, jet pressure,

microabrasive concentration, jet angle and microabrasive particle size are investigated comprehensively. Moreover, the processing effects with GSC and SD as the abrasives are compared and the mechanisms of these two different processing techniques are discussed.

## Materials and Methods

Figure 1 shows the schematic diagram of M-MDJM processing system. The abrasive is blended with water in the storage tank to prevent the aggregation and sedimentation. The compressed air from the air compressor flows into two ways after the globe valve. One way flows through the pressure maintaining valve, the throttle valve and the globe valve, sequentially, then inhale the mixture of water and microabrasive particles to form the high-speed multiphase jet flow through the nozzle; the other way of the air flows through the globe valve to the vacuum generator, which is used to suck out the microabrasive particles and water from the processing tank and back to the storage tank eventually, so as to realize the recycling of microabrasive particles.

The nozzle is one of the most critical parts of the experimental system. Its shape, size and stability play a vital role in machining effect.<sup>[20]</sup> Depending on the purpose and the machining conditions, a special nozzle is designed to realize sustainable supply of microabrasive. The nozzle is made of hard alloy which mainly includes an entrance section, an inner venturi tube, a mixing chamber and a focus tube, and its outlet diameter is about 1.3 mm. The negative pressure is formed inside the nozzle when the compressed air flow through the nozzle with high-speed; the mixture is inhaled into the mixing chamber, and then, mixed with compressed air, accelerated to form the multi-phase microabrasive jet flow toward the workpiece.

To overcome the disadvantages of GSC, a harder material, synthetic diamond (SD), is used as microabrasive in this research. The SD powder of different mesh numbers between 800 and 3000 are selected. The corresponding relationship between mesh size and particle diameter is shown in Table 1.

Figure 2(a) presents the SEM image of the typical SD particles with the average diameter around 13  $\mu\text{m}$ . To fabricate the surface texture with proper shape and size at particular location, a mask with certain abrasion resistance and relative thickness is designed and fixed upon the workpiece.

Figure 2(b) shows a typical mask of 304 stainless steel sheet (thickness of 0.2 mm) of fabricated rectangular array with a dimension of  $3.3 \times 0.5 \text{ mm}$  via laser machining. To investigate the processing technic and efficiency of the multiphase jet machining, the finish depths of the machining regions under different experimental conditions are measured for the sake of comparison in the following sections.

As shown in Fig. 2(c), the nozzle is driven to move in a S-type path across the unmasked area by two stepper motors with the XY stages. The jet distance is controlled by the Z axis stepper motor. In this research, the relative speed of the nozzle

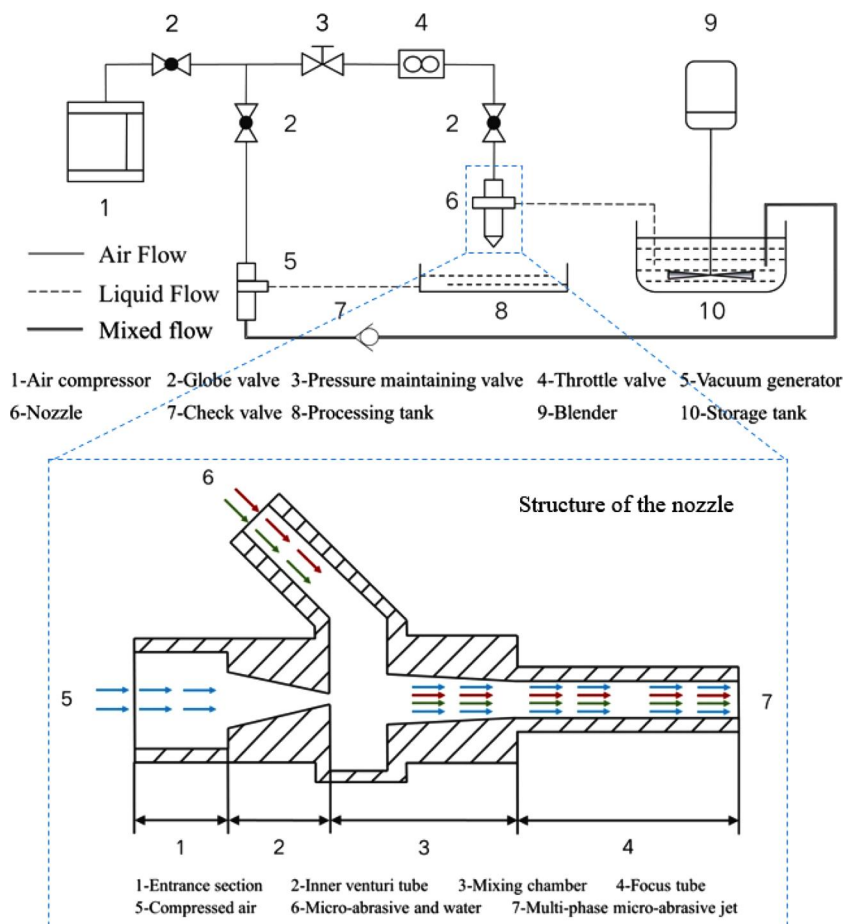


Figure 1. Schematic diagram of processing system.

**Table 1.** The corresponding relationship between mesh number and particle diameter.

Mesh number	3000	2000	1500	1200	1000	800
Grain diameter, $\mu\text{m}$	4.5	6.5	8	10	13	18

and the workpiece is 0.8 mm/s and the feed distance was 0.1 mm to ensure the uniformity of processing.

Silicon carbide is a commonly used material of mechanical seal end face.<sup>[21]</sup> It's of high hardness, good wear resistance, low chemical activity, and good heat resistance. In this research, reaction-bonded silicon carbide (RBSC) is used as the material of workpiece. The main physical properties of SD and RBSC are compared in Table 2. The machined surfaces were evaluated by a scanning electron microscope (HITACHI, Japan) and a 3D optical profilometer (Bruker, USA). The surface roughness is measured on a rectangle area of  $1122 \mu\text{m}^2$  on the groove bottom.

## Results and Discussion

To compare the processing results of different microabrasive materials, GSC and SD of the same abrasive size were chosen to process the RBSC. The processing conditions are jet pressure of 0.6 MPa, jet angle of  $90^\circ$ , jet distance of 12 mm, abrasive concentration of 10%, and abrasive size of  $13 \mu\text{m}$ . Since a big difference exists for the processing efficiency between GSC and SD, after repeated attempts, the processing time was fix as 128 and 4 min, respectively.

The processing result of GSC abrasive is shown in Fig. 3(a). After 128 min of processing, although the average depth is  $10.4 \mu\text{m}$  and the bottom surface roughness is  $1.79 \mu\text{m}$ , there are still some spikes in the microgrooves. The top of these spikes is almost as high as the unprocessed surface, just like "isolated islands" in the processing area.

The processing result of SD abrasive is shown in Fig. 3(b). After 4 min of processing, the average depth is  $49.3 \mu\text{m}$  and the bottom surface roughness is only  $0.59 \mu\text{m}$ . Obviously, the bottom of the groove looks smooth, and there is no "isolated islands" on the processed area. It also can be found that the

machining speeds are different for different abrasives. While GSC is used, the ratio of groove depth over machining time is  $0.0812 \mu\text{m}/\text{min}$ ; while using SD as the microabrasive, the ratio of groove depth over machining time is  $12.3 \mu\text{m}/\text{min}$ . The results show that the processing efficiency of SD is 141.9 times that of GSC, and the machining consistency of SD is better.

These results might be due to the different processing mechanisms when using different materials as microabrasive.

When GSC is used as the microabrasive, the microabrasive material is the same as the processed workpiece, so the indentation theory can be used as the erosion model for RBSC.<sup>[22]</sup> Figure 4 presents a diagram of solid particle impact mechanism. When the abrasive tip is pressed into the surface, a plastic zone will be induced under the indent. In the vertical direction, radial cracks will be generated, which will affect the surface roughness and strength of machined surface. Lateral cracks will be generated in the horizontal direction of plastic zone, which is the main reason for the material of workpiece to be removed. During M-MAJM processing, the GSC abrasive particles impact the RBSC surface may produce more radial cracks rather than lateral cracks. With the deepening and expansion of the radial crack, several micropits and microprotrusion will appear in the processing area, which leads to high surface roughness and appear the phenomenon of "isolated island" on the groove bottom.

When using micro SD as microabrasive material, the hardness of SD is higher than that of RBSC, so the machining process could be the continuous cutting process of RBSC by SD. Therefore, the processing efficiency is higher, and the processing consistency is better.

The related research<sup>[17,23]</sup> have reported that the jet distance, jet pressure, jet angle, abrasive concentration and the particle size of microabrasive are of significant influence on machining effect. Hence, experiments were performed to investigate the influence of these parameters on the processing results.

Figure 5 presents the influence of jet distance on the depth and surface roughness. The experimental conditions are the

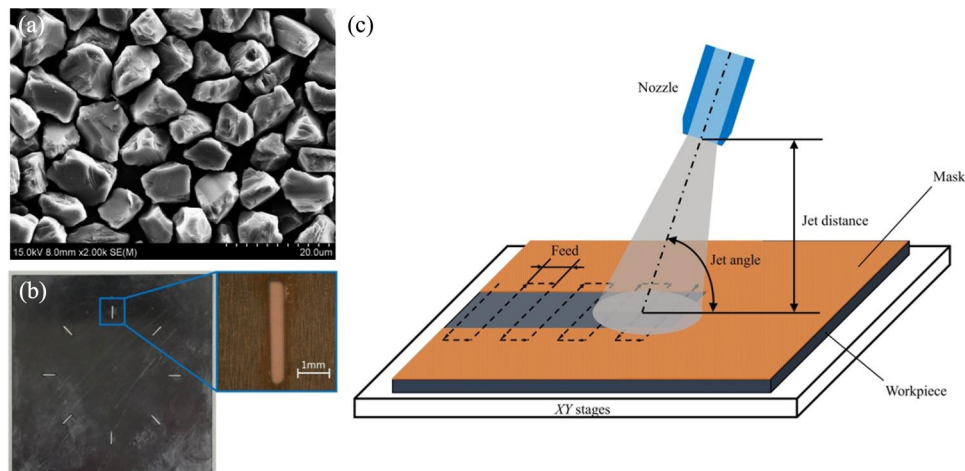


**Figure 2.** (a) SEM image of SD particles (mesh number: 1000); (b) the mask made of stainless steel; and (c) schematic diagram of the S-type processing path. Note: SD, synthetic diamond.

**Table 2.** The physical properties of SD and RBSC.

Materials	Density $\rho$ , g/cm <sup>3</sup>	Hardness	Modulus of elasticity $E$ , GPa	Tensile strength $\sigma_b$ , MPa
SD	3.52	HV 1000	1100	1050–3000
RBSC	3.05	HRA 91	330	352

SD, synthetic diamond; RBSC, reaction-bonded silicon carbide.

same including the jet angle of 90°, jet pressure of 0.6 MPa, abrasive concentration of 10% and abrasive size of 13  $\mu\text{m}$ . It can be found that the groove depth was relative short and the surface roughness was high while the jet distance was either too short or too long. The groove depth achieved the maximum when jet distance is 12 mm, and the surface roughness reaches the minimum when jet distance is 9 mm at above experimental condition, indicating that 9–12 mm is the preferable jet distance range.

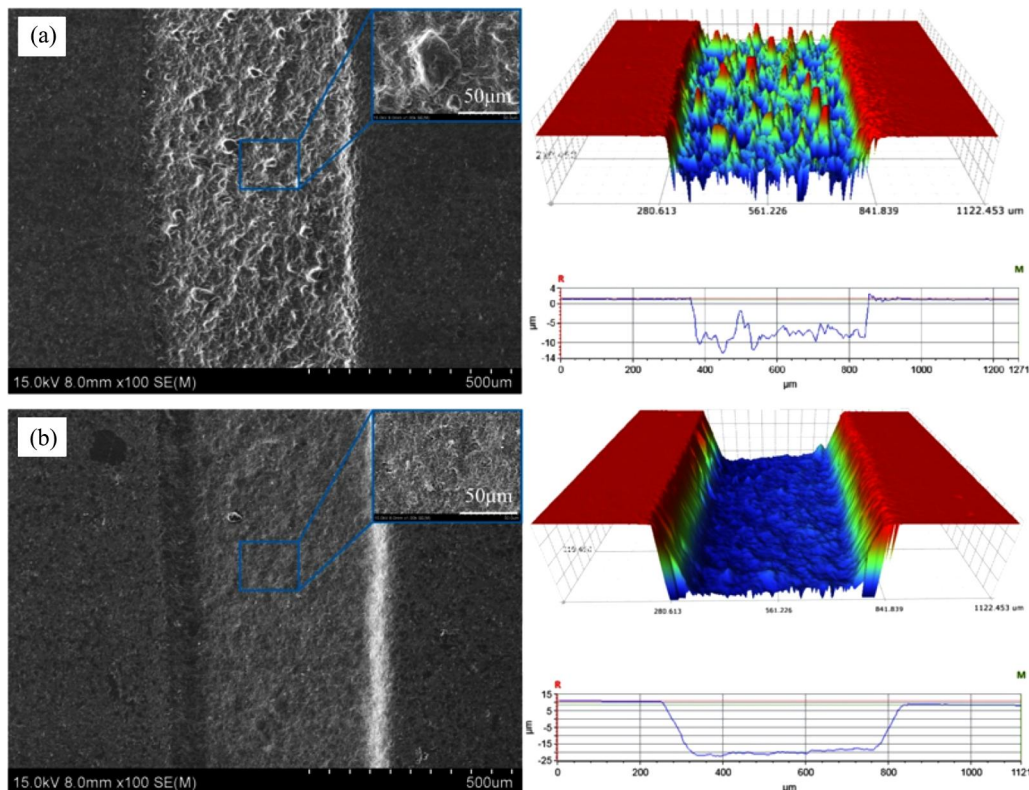
The jet flow diverges after the nozzle exit, the longer the distance, the more divergent. While jet distance is short, the jet flow is relative thin, and abrasive particles will be gathered and concentrated on a small processing surface area, so that the collision between the abrasive particles might happen frequently, and the kinetic energy of the particles is decreased. Consequently, the machining efficiency is reduced. On the other hand, while the jet distance is longer than 12 mm, the multiphase jet is dispersed too much, which leads to the reduction of the processing efficiency.

Figure 6 shows the effect of jet pressure on the depth and surface roughness under the conditions of jet angle 90°, jet distance 12 mm, microabrasive concentration 10% and abrasive size 13  $\mu\text{m}$ . The groove was shallow while air pressure was

0.3 MPa. With the increase of jet pressure, the machined depth increased almost linearly. This phenomenon could be simply explained that abrasive particles will get higher speed and kinetic energy with higher jet pressure, hence, higher machining efficiency could be obtained. However, as the jet pressure increases to 0.4 MPa, the surface roughness also has an obvious increasing, fortunately, when the jet pressure is higher than 0.4 MPa, the surface roughness can stay stable relatively, providing a stable processing condition.

The effect of different abrasive concentration on the processing is shown in Fig. 7, while the jet angle is 90°, the jet pressure is 0.6 MPa, the abrasive size is 13  $\mu\text{m}$ , and the jet distance is 12 mm. Table 3 shows the abrasive flow rates under different abrasive concentration. The results show that the groove depth increases with the increasing abrasive concentration. The reason could be that the quantity of microabrasive particles per second is increased, which improves the processing speed. However, the machining efficiency (defined as the ratio of groove depth over abrasive flow rate) of a unit mass of microabrasive is increased first and then decreased, and the maximum value is reached when the abrasive concentration is 5%. Meanwhile, the surface roughness reaches the minimum value. Therefore, different abrasive concentrations should be chosen for different processing requirements. In a certain range, higher processing speed can be achieved with higher abrasive concentration; when the abrasive concentration is 5%, high surface quality and machining efficiency of a unit mass of microabrasive can be achieved.

The nozzle vertically spraying to the workpiece, i.e., jet angle equaling to 90°, is the simplest setting. Tsai et al.<sup>[24]</sup> have



**Figure 3.** Typical processing results by different abrasives of (a) GSC abrasive and (b) SD abrasive. Note: GSC, green silicon carbide; SD, synthetic diamond.

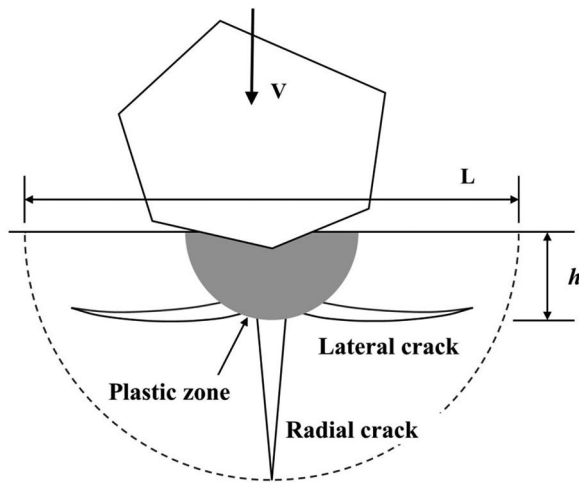


Figure 4. The schematic diagram of solid particle impact.

reported that when the jet angle is less than  $60^\circ$ , the material removal rate is low and the jet machining process is often used as a polishing process. In this paper, the effect of M-MDJM on the jet angle of  $90^\circ$ – $70^\circ$  is studied and compared. The processing conditions are the jet distance of 12 mm and the microabrasive concentration of 10%. The SD abrasives with the mesh number from 800# to 3000# were used in the experiments.

Figure 8 shows the effect of microdiamond abrasive particles with different particle sizes and different jet angles. It is found SD#3000 abrasive, the smallest particle in this study, obtained the lowest machining efficiency; although the experiment data varies in a certain rang, generally, the efficiency increases when the particle size increases. This can be simply explained that large particle will have high abrasive ability. However, with large particles, the surface roughness also increased. Therefore, similar to the grinding process, abrasive

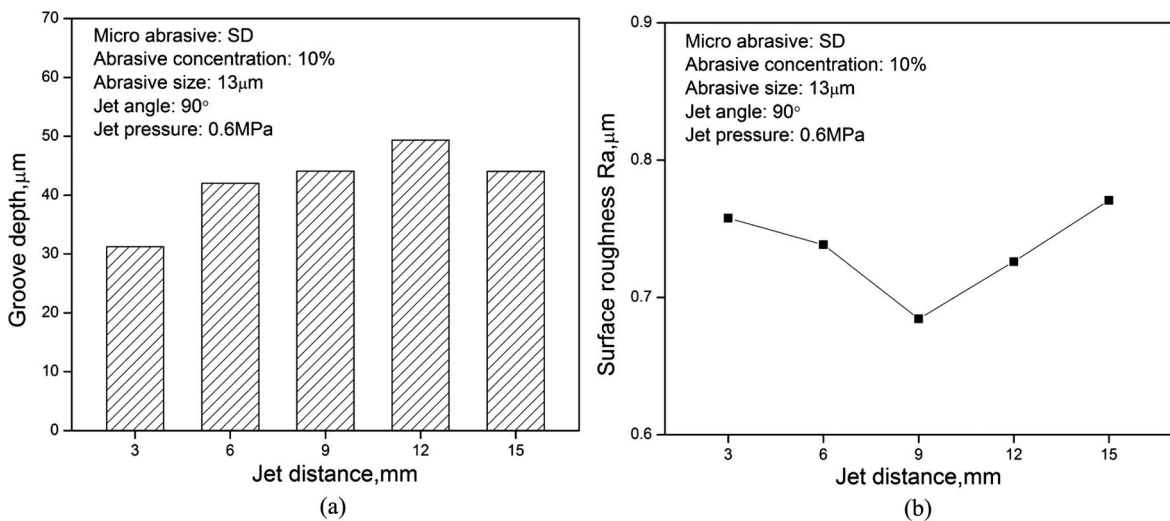


Figure 5. The effect of jet distance on (a) groove depth and (b) surface roughness.

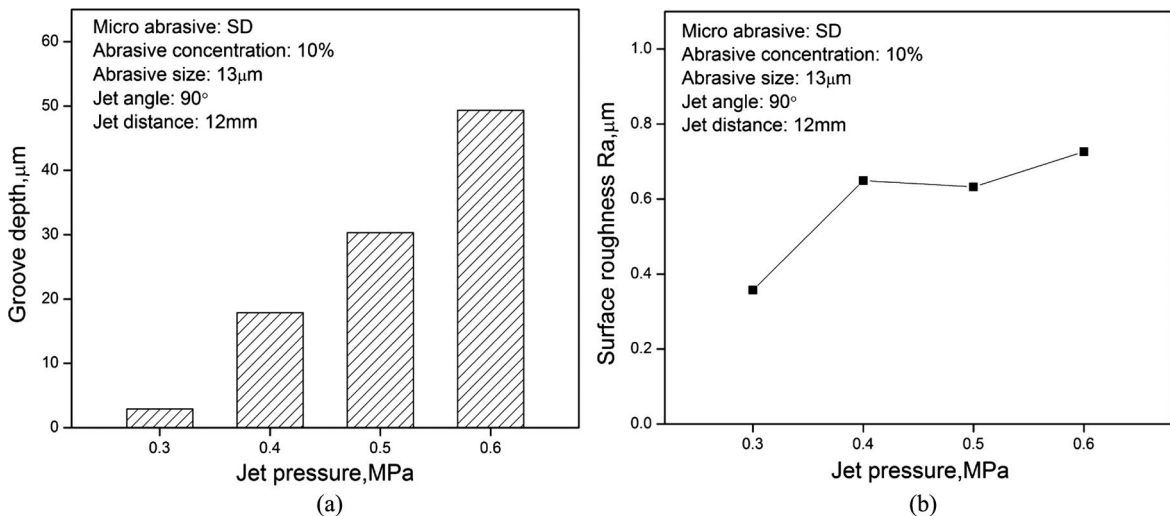


Figure 6. The effect of jet pressure on (a) groove depth and (b) surface roughness.

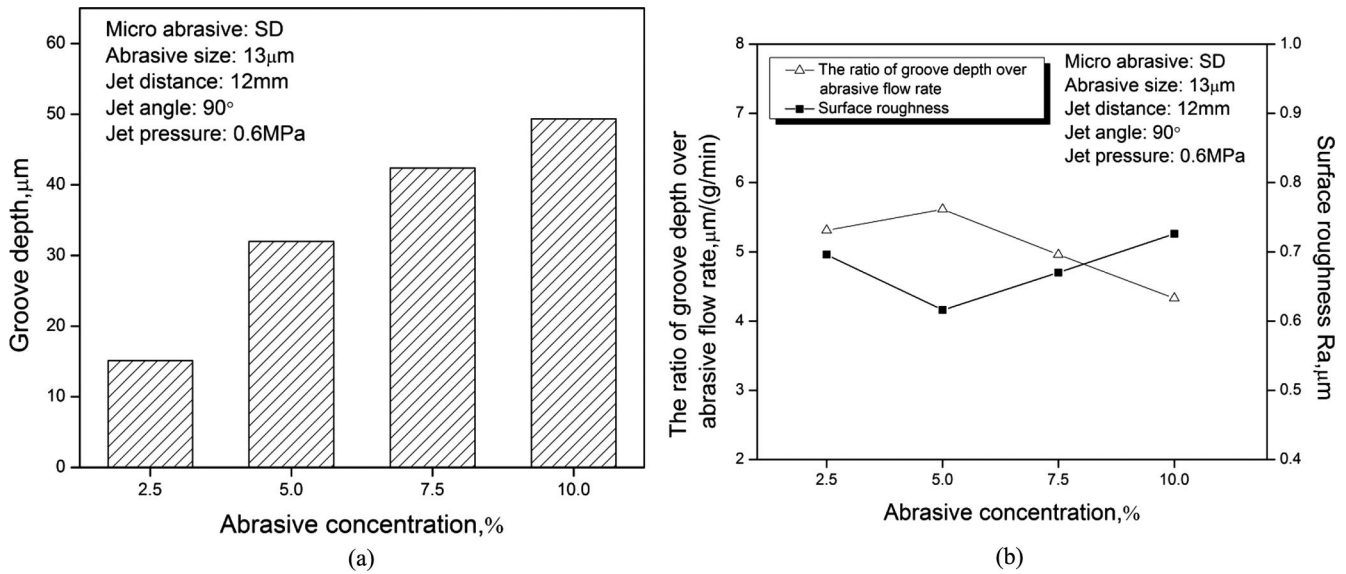


Figure 7. The effect of abrasive concentration on (a) groove depth and (b) surface roughness and the ratio of groove depth over abrasive flow rate.

Table 3. The abrasive flow rates under different abrasive concentration.

Abrasive concentration (mass fraction) (%)	2.5	5	7.5	10
Abrasive flow rates (g/min)	2.85	5.70	8.55	11.40

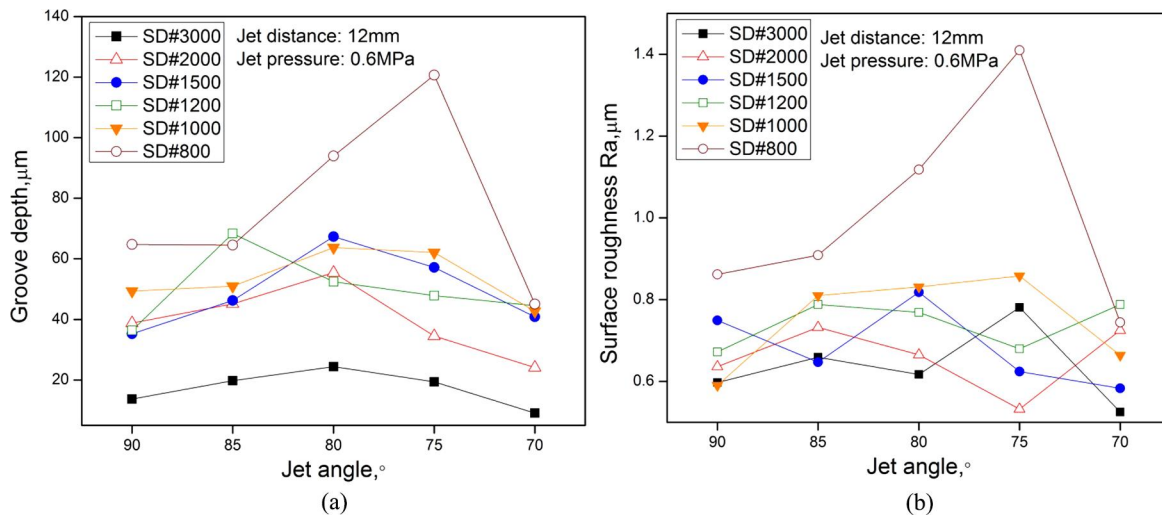


Figure 8. The effect of jet angle on (a) groove depth and (b) surface roughness.

selection is a compromised issue of machining efficiency and surface roughness.

For the effect of jet angle, the processing efficiency on the jet angle between 85° and 75° is higher than that of 90°, this phenomenon is more obvious when the microabrasive mesh number is 800. When the jet angle is reduced to 70°, the processing efficiency begins to decrease, and so does the surface roughness. The main reason may be that the inclined nozzle will provide horizontal velocity of the microabrasive, which leads to the effect of scratch of SD particles on the surface of RBSC, so that the material removal efficiency is increased. However, inclined jet is easier to disperse accumulated microabrasive particles and reduce the mutual impact

between the particles, reducing the kinetic energy loss of particles consequently.

### Conclusion

A processing technology of multiphase jet machining using microdiamond abrasive was developed for the surface texturing on the RBSC (SiC) surfaces. Experiments were concentrated on the effects of process parameters and reasonable mechanism were proposed. The conclusions drawn from this study are as follows:

1. The multiphase microdiamond abrasive jet machining can be used in processing RBSC under the condition of relative

low jet pressure. Compare to the processing results of GSC, the processing efficiency of synthetic diamond is 141.9 times that of GSC under the same processing conditions. Additionally, the bottom surface roughness of the micro-grooves is lower and the phenomenon of “isolated island” is disappeared.

2. The multiphase microdiamond abrasive jet machining can be used to fabricate surface texture of mechanical seals efficiently. The processing effect is related to the factors such as the jet distance, jet pressure, abrasive concentration, jet angle, and abrasive size. Rational selection of machining parameters can improve the processing efficiency.
3. The processing effect of multiphase microdiamond abrasive jet machining under different jet angles was compared. Under the same experimental conditions, reducing the jet angle appropriately can improve the processing efficiency significantly.

## Funding

This work was financially supported by the National Nature Science Foundation of China (NSFC) (Grant No. 51675268), Natural Science Foundation of Anhui Province of China (1708085QE113), Natural Science Research of Higher Education of Anhui Province (KJ2016A093, KJ2016A813).

## References

- [1] Nau, B. S. Research in Mechanical Seals. *J. Mech. Eng. Sci.* **1990**, *204*, 349–376.
- [2] [https://en.Wikipedia.Org/wiki/end\\_face\\_mechanical\\_seal](https://en.Wikipedia.Org/wiki/end_face_mechanical_seal). (End face mechanical seal section).
- [3] Wang, X. L.; Adachi, K.; Otsuka, K.; Kato, K. Optimization of the Surface Texture for Silicon Carbide Sliding in Water. *Appl. Surf. Sci.* **2006**, *253*, 1282–1286.
- [4] Yu, H.; Huang, W.; Wang, X. Dimple Patterns Design for Different Circumstances. *Lubr. Sci.* **2013**, *25*, 67–78.
- [5] Shi, L.; Wang, X.; Su, X.; Huang, W.; Wang, X. Comparison of the Load-Carrying Performance of Mechanical Gas Seals Textured with Microgrooves and Microdimples. *J. Tribol.* **2015**, *138*, 88–90.
- [6] Qian, S.; Ji, F.; Qu, N.; Li, H. Improving the Localization of Surface Texture by Electrochemical Machining with Auxiliary Anode. *Mater. Manuf. Processes* **2014**, *29*, 1488–1493.
- [7] Ibatan, T.; Uddin, M. S.; Chowdhury, M. A. K. Recent Development on Surface Texturing in Enhancing Tribological Performance of Bearing Sliders. *Surf. Coat. Technol.* **2015**, *272*, 102–120.
- [8] Uthayakumar, M.; Khan, M. A.; Kumaran, S. T.; Slota, A.; Zajac, J. Machinability of Nickel-Based Superalloy by Abrasive Water Jet Machining. *Mater. Manuf. Processes* **2016**, *31*, 1733–1739.
- [9] Yuvaraj, N.; Kumar, M. P. Multiresponse Optimization of Abrasive Water Jet Cutting Process Parameters using Topsis Approach. *Mater. Manuf. Processes* **2015**, *30*, 882–889.
- [10] Karakurt, I.; Aydin, G.; Aydin, K. An Experimental study on the Depth of Cut of Granite in Abrasive Waterjet Cutting. *Mater. Manuf. Processes* **2012**, *27*, 538–544.
- [11] Nair, A.; Kumanan, S. Multi-Performance Optimization of Abrasive Water Jet Machining of Inconel 617 using WPCA. *Mater. Manuf. Processes* **2017**, *32*, 693–699.
- [12] Yuvaraj, N.; Kumar, M. P. Investigation of Process Parameters Influence in Abrasive Water Jet Cutting of d2 Steel. *Mater. Manuf. Processes* **2017**, *32*, 151–161.
- [13] Park, D. S.; Cho, M. W.; Lee, H.; Cho, W. S. Micro-Grooving of Glass using Micro-Abrasive Jet Machining. *J. Mater. Process. Technol.* **2004**, *146*, 234–240.
- [14] Wakuda, M.; Yamauchi, Y.; Kanzaki, S. Material Response to Particle Impact During Abrasive Jet Machining of Alumina Ceramics. *J. Mater. Process. Technol.* **2003**, *132*, 177–183.
- [15] Nouraei, H.; Wodoslawsky, A.; Papini, M.; Spelt, J. K. Characteristics of Abrasive Slurry Jet Micro-Machining: A Comparison with Abrasive Air Jet Micro-Machining. *J. Mater. Process. Technol.* **2013**, *213*, 1711–1724.
- [16] Naresh Babu, M.; Muthukrishnan, N. Investigation on Surface Roughness in Abrasive Water-Jet Machining by the Response Surface Method. *Mater. Manuf. Processes* **2014**, *29*, 1422–1428.
- [17] Getu, H.; Ghobeity, A.; Spelt, J. K.; Papini, M. Abrasive Jet Micro-machining of Acrylic and Polycarbonate Polymers at Oblique Angles of Attack. *Wear* **2008**, *265*, 888–901.
- [18] Tsai, F. C.; Yan, B. H.; Kuan, C. Y.; Huang, F. Y. A Taguchi and Experimental Investigation into the Optimal Processing Conditions for the Abrasive Jet Polishing of SKD61 Mold Steel. *Int. J. Mach. Tools Manuf.* **2008**, *48*, 932–945.
- [19] Su, X.; Shi, L.; Huang, W.; Wang, X. A Multi-Phase Micro-Abrasive Jet Machining Technique for the Surface Texturing of Mechanical Seals. *Int. J. Adv. Manuf. Technol.* **2016**, *86*, 2047–2054.
- [20] Wang, R.; Wang, M. A Two-Fluid Model of Abrasive Waterjet. *J. Mater. Process. Technol.* **2010**, *210*, 190–196.
- [21] Chen, C.-Y.; Chung, C.-J.; Wu, B.-H.; Li, W.-L.; Chien, C.-W.; Wu, P.-H.; Cheng, C.-W. Microstructure and Lubricating Property of Ultra-Fast Laser Pulse Textured Silicon Carbide Seals. *Appl. Phys. Mater. Sci. Process.* **2012**, *107*, 345–350.
- [22] Malkin, S.; Hwang, T. W. Grinding Mechanisms for Ceramics. *Cirp Ann. Manuf. Technol.* **1996**, *45*, 569–580.
- [23] Balasubramaniam, R.; Krishnan, J.; Ramakrishnan, N. A Study on the Shape of the Surface Generated by Abrasive Jet Machining. *J. Mater. Process. Technol.* **2002**, *121*, 102–106.
- [24] Tsai, F.-C.; Yan, B.-H.; Kuan, C.-Y.; Hsu, R.-T.; Hung, J.-C. An Investigation into Superficial Embedment in Mirror-Like Machining using Abrasive Jet Polishing. *Int. J. Adv. Manuf. Technol.* **2009**, *43*, 500–512.